Nanotoxicology

ISSN: 1743-5390 (Print) 1743-5404 (Online) Journal homepage: https://www.tandfonline.com/loi/inan20

Research on the hepatotoxicity mechanism of citrate-modified silver nanoparticles based on metabolomics and proteomics

Jiabin Xie, Wenying Dong, Rui Liu, Yuming Wang & Yubo Li

To cite this article: Jiabin Xie, Wenying Dong, Rui Liu, Yuming Wang & Yubo Li (2018) Research on the hepatotoxicity mechanism of citrate-modified silver nanoparticles based on metabolomics and proteomics, Nanotoxicology, 12:1, 18-31, DOI: 10.1080/17435390.2017.1415389

To link to this article: https://doi.org/10.1080/17435390.2017.1415389

NANOTOXICOLOGY, 2018
VOL. 12, NO. 1, 18–31
https://doi.org/10.1080/17435390.2017.1415389

Taylor & Francis
Taylor & Francis Group

ARTICLE

Research on the hepatotoxicity mechanism of citrate-modified silver nanoparticles based on metabolomics and proteomics

Jiabin Xie[a]*, Wenying Dong[a]*, Rui Liu[b], Yuming Wang[a] and Yubo Li[a]

[a]Tianjin State Key Laboratory of Modern Chinese Medicine, School of Traditional Chinese Materia Medica, Tianjin University of Traditional Chinese Medicine, Tianjin, PR China; [b]School of Chinese Materia Medica, Shanxi University of Traditional Chinese Medicine, Shanxi, PR China

ABSTRACT

Citrate-modified silver nanoparticles (AgNP-cit) have received extensive attention due to their excellent antimicrobial properties. However, these particles tend to migrate *in vivo*, thereby entering the blood circulatory system in granular form and accumulating in the liver, causing toxic reactions. However, the mechanism underlying AgNP-cit toxicity is not yet clear. Thus, we adopted a tandem mass tag (TMT)-labeled quantitative proteomics and metabolomics approach to identify proteins and small molecule metabolites associated with AgNP-cit-induced liver damage and constructed interaction networks between the differentially expressed proteins and metabolites to explain the AgNP-cit toxicity mechanism. AgNP-cit resulted in abnormal purine metabolism mainly by affecting xanthine and other key metabolites along with pyruvate kinase and other bodily proteins, leading to oxidative stress. AgNP-cit regulated the metabolism of amino acids and glycerol phospholipids through glycerol phospholipids, CYP450 enzymes and other key proteins, causing liver inflammation. Via alanine, isoleucine, L-serine dehydratase/L-threonine deaminase and other proteins, AgNP-cit altered the metabolism of glycine, serine and threonine, cysteine and methionine, affecting oxidation and deamination, and ultimately leading to liver damage. This work clearly explains toxic reactions induced by AgNP-cit from three perspectives, oxidative stress, inflammatory response, and oxidation and deamination, thus providing an experimental basis for the safe application of nanomaterials.

ARTICLE HISTORY
Received 19 June 2017
Revised 4 December 2017
Accepted 5 December 2017

KEYWORDS
Citrate-modified silver nanoparticles; systems biology analysis; UPLC/Q-TOF-MS

Introduction

With the widespread use of nanomaterials, silver nanoparticles have also received extensive attention, and they are often coated with citrate to promote stability and avoid aggregation. Furthermore, citrate can be quickly decomposed by the liver and excreted through the kidneys and is not toxic by itself (Khadzhynov et al. 2014; Bastos et al. 2016). However, citrate-modified silver nanoparticles (AgNP-cit) have a tendency to migrate *in vivo*; They enter the blood circulatory system in granular form and accumulate in the liver, causing toxic reactions (Agnihotri, Mukherji, and Mukherji 2014; Jiménez-Lamana et al. 2014; Wei et al. 2015). However, the mechanism underlying the hepatotoxicity of AgNP-cit is not clear; Thus, to make silver nanoparticles and other nano materials safe and to achieve reasonable applications to avoid toxic side effects, an in-depth, systematic assessment of the silver nanoparticles toxicity mechanism is required.

Proteomics explores the pathogenesis of diseases at the protein level by qualitatively and quantitatively analyzing all the proteins expressed by a cell or organism under different environmental conditions (Lavatelli and Merlini 2016). Specifically, quantitative proteomics using the stable isotope labeling method has advantages, such as accuracy, reliability, high throughput, and good repeatability. Metabolomics is the study of the composition and variation of metabolic groups, thereby revealing the overall metabolic response and dynamic changes in the body's response to a variety of internal and external factors (Bai et al. 2014; Stringer et al. 2016). Proteomic and metabolomic analyses are used to analyze and validate differential proteins and metabolites and to understand changes in toxicity from an

CONTACT Yubo Li yaowufenxi001@sina.com Tianjin State Key Laboratory of Modern Chinese Medicine, School of Traditional Chinese Materia Medica, Tianjin University of Traditional Chinese Medicine, 312 Anshan west Road, Tianjin 300193, PR China
*Co-first authors: Jiabin Xie and Wenying Dong.

Supplemental data for this article can be accessed here.

overall perspective, thus contributing to the elucidation of molecular toxicity mechanisms. Currently, studies on the effects of silver nanoparticles on the liver, mainly evaluating mechanisms involved in oxidative stress and apoptosis, using single proteomics or metabolomics methods have been reported. However, these studies focus on only the toxic effects of silver nanoparticles at the cellular level (Hussain et al. 2005; Piao et al. 2011). We know that cells by themselves cannot replace an entire animal, toxicity mechanisms cannot be systematically explained by *in vitro* cell studies. Therefore, in this research, we studied the toxic characteristics of silver nanoparticles at the proteomics and metabolomics levels using a high-throughput holistic animal research model. Not only do we now fully understand changes in the laws of proteins and metabolites in the occurrence and development of liver damage, but we also panoramically reveal the mechanism of toxicity, which provides an experimental basis for toxic warnings, diagnosis, treatment, and evaluation.

In this study, the mechanism of citrate-modified silver nanoparticles-induced liver injury was elucidated by TMT-labeled quantitative proteomics and metabolomics methods. First, a proteomics approach was used to comprehensively evaluate the biological effects of AgNP-cit and to screen for differentially expressed proteins associated with liver injury. Second, metabolomics was used to screen for possible metabolites that may be associated with liver damage. Finally, the differentially expressed proteins and metabolites were integrated and analyzed, and the metabolic pathways were screened to elucidate the toxicity mechanism of AgNP-cit in liver injury. This study is of great significance to elucidation of the AgNP-cit toxicity mechanism and to the rational application of nanomaterials.

Materials and methods

Characterization of citrate-modified silver nanoparticles

Citrate-modified silver nanoparticles were purchased from Shanghai Pan-Tian Powder Technology Co., Ltd., Shanghai, China, and the company provided technical support. AgNP-cit were characterized by transmission electron microscopy (Figure 1).

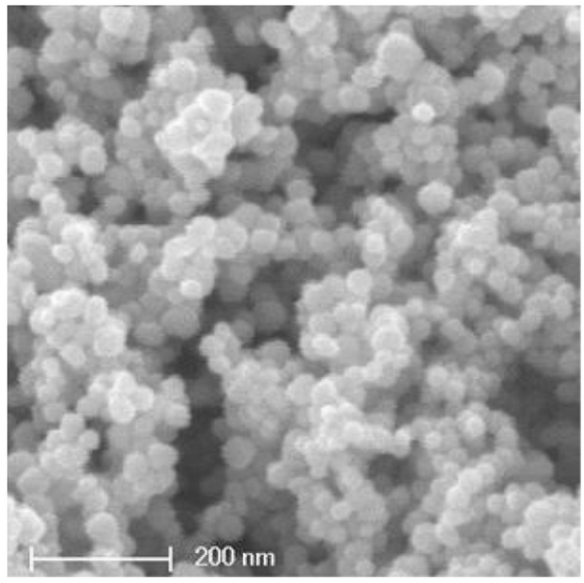

Figure 1. The electron microscope of AgNP-cit is provided by Shanghai Pan-Tian Powder Technology Co., Ltd, Shanghai, China. AgNP-cit has a particle size range of 10–30 nm. The average particle size is 20 nm. The particles are spherical, uniform dispersion and the scale is 200 nm.

Experimental design

Male Wistar rats weighing 200 ± 20 g were provided by Sibei Fu (Beijing, China) Experimental Animal Science and Technology Co., Ltd. [SCXK (Jing) 2011-0004], and housed at the Experimental Animal Center of Tianjin Institute of Radiology animal laboratory in SPF conditions. The rats were raised in controlled environmental conditions with a room temperature of 23 ± 2 °C, a relative humidity of 35 ± 5%, and a light-dark cycle of 12 h. After a week of adaptation, the animal experiments were carried out. The rats were randomly divided into two groups: a control group and an AgNP-cit group. The rats in each group were given adequate water and food. The experimental group and the dose each group received are shown in Table 1 (Tiwari, Jin, and Behari 2011). A flow chart of studies on the AgNP-cit toxicity mechanism is provided in Figure 2. The materials and reagents used in this experiment are described in the supplementary materials.

Sample collection and treatment

Blood samples (5 mL) from rats in each group were collected via abdominal aorta blood draws 4 weeks after administration (Qin et al. 2017). Whole blood was centrifuged at 3500 rpm at 4 °C for 10 min to isolate the serum, which was stored at −80 °C for

Table 1. The experimental group and dose of each group.

Grouping	Quantity	Dose	Mode of administration	Modeling time
Control group	9	10 mL/kg/d	Physiological saline, gavage, continuous administration	4 weeks
AgNP-cit group	9	40 mg/kg/d	AgNP-cit, gavage, continuous administration	4 weeks

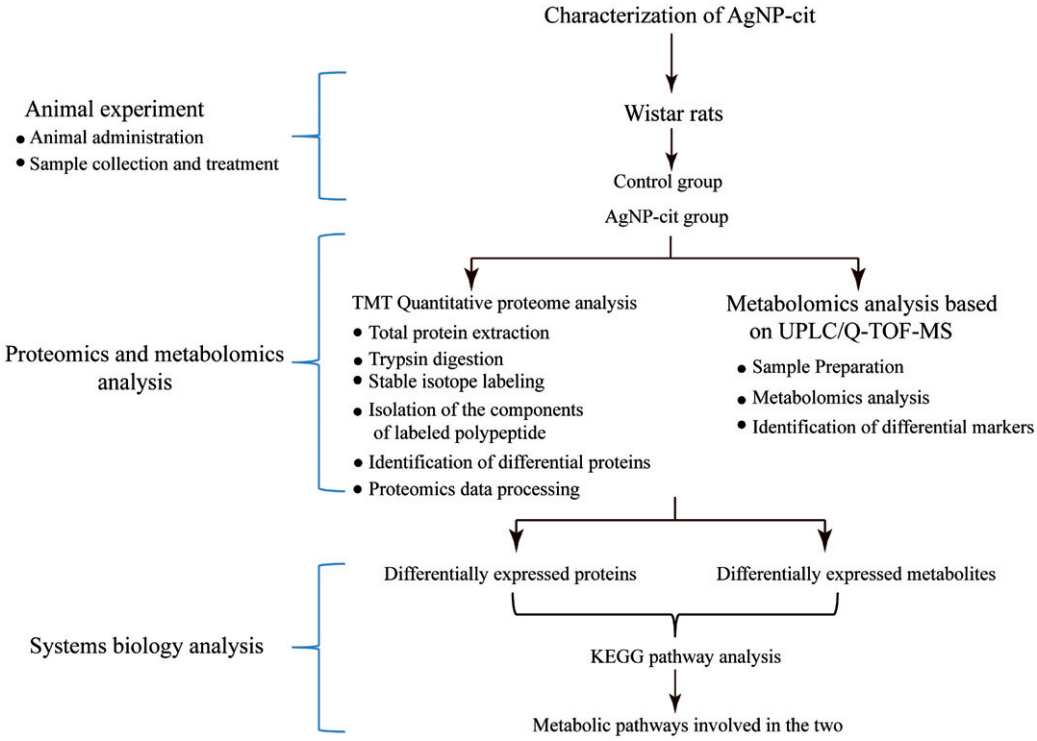

Figure 2. Flow chart of toxicity mechanism of AgNP-cit.

subsequent biochemical analyses (Li et al. 2016). Each group was sacrificed 4 weeks after administration; the same portion of each liver was quickly removed, perfused with cold PBS to remove blood, immediately frozen in liquid nitrogen for 5 min, and then stored at −80 °C for proteomic and metabolic analyses (Kuzmanov et al. 2016). The same portion of the liver was taken from each group, and blood stains were washed with saline. The liver tissues were then immersed in 10% formaldehyde solution for hematoxylin and eosin (H&E) staining (Li et al. 2016; Recordati et al. 2016).

Proteomics research

Tissue sample preparation

A liver was removed from −80 °C storage, rinsed free of liquid nitrogen, and thoroughly ground into powder. Four volumes of lysis buffer (8 M urea, 1% protease inhibitor and 2 mM EDTA) were added, and the cells were ultrasonically cracked. The sample was centrifuged at 12 000 *g* at 4 °C for 10 min (Kuzmanov et al. 2016), and the protein concentration was measured using a bicinchoninic acid (BCA) kit. Dithiothreitol was added to the protein solution, reduced at 56 °C for 30 min. Iodoacetamide was then added, and the mixture was incubated at room temperature for 15 min. Trypsin was added at a mass ratio of 1:50 (trypsin:protein) and eluted at 37 °C overnight. Then, trypsin was added again at a 1:100 mass ratio (trypsin:protein) for 4 h (Xu et al. 2016). After trypsin digestion, the peptide was desalted using a Strata X C18 SPE column (Phenomenex) and vacuum-dried. The peptide was digested with 0.5 M TEAB and labeled according to the TMT kit instructions (Licker et al. 2014). The specific TMT labeling information is presented in Table S1.

Mass spectrometry quality control test

The MS quality control test was performed by detecting the mass error of all the identified peptides. See the supplementary material for details.

Data processing

Details regarding high performance liquid chromatography (HPLC) fractionation and the proteomic map obtained by liquid chromatography-tandem mass spectrophotometry (LC-MS/MS) analysis are described in the supplementary materials. Secondary MS data were retrieved using MaxQuant version 1.5.2.8 (Max Planck Institute of Biochemistry, Planegg, Germany), and the retrieve parameter settings are described below. The Uniprot Rat database was used, and an anti-library was added to calculate the false discovery rate (FDR) caused by random matching. The cut mode was set to Trypsin/P, and the number of cutoff points was set to 2. The minimum length of the peptide was set to 7 amino acid residues, and the maximum number of modifications for peptides was 5. The tolerances of the first parent ion mass error of the First search and Main search were 20 and 5 ppm, respectively. Furthermore, the mass error tolerance of the secondary fragment ion was 0.02 Da. The quantitative method was set to TMT-6plex, and the FDRs of protein identification and PSM identification were set to 1% (Xu et al. 2016).

Metabolomics research

Tissue sample preparation

Liver tissue samples frozen at −80 °C were removed and thawed at room temperature. Then, 100 mg of liver tissue was weighed, and 500 μL of methanol was added. The mixture was homogenized at 3000 rpm for 30 s at 0 °C and centrifuged at 12 000 rpm for 10 min at 4 °C. The supernatant (150 μL) was taken from the vial and the lower layer was extracted with 125 μL of chloroform, 250 μL of methanol, and 125 μL of water for the second extraction. The mixture was homogenized at 3000 rpm for 30 s at 0 °C and centrifuged at 12 000 rpm for 10 min at 4 °C. Then, 150 μL of the supernatant was collected in the previous corresponding vial (Lin 2008). Meanwhile, liver tissue samples were weighed from each group, and the total weight in the centrifuge tube was about 100 mg. The quality control (QC) samples were then prepared as described above. In addition, ultra-performance liquid chromatography with quadrupole time-of-flight mass spectrometry (UPLC/Q-TOF-MS) was used for injection analysis and the specific analysis conditions are described in the supplementary materials (Table S2).

Mass spectrometry quality control test

The MS quality control test was performed using the instrument precision, method precision, sample stability, and other methods. Details are provided in the supplementary material.

Data processing

In this study, the UPLC/Q-TOF-MS technique was used to analyze the liver of the rat liver toxicity model induced by AgNP-cit. The specific data processing process was as follows: original data was collected by Masslynx version 4.1 software (Waters Corp., Milford, MA) in the workstation and SIMCA-P^+ version 11.5 statistical software (Umetrics AB, Umeå, Sweden) was used for multivariate statistical analysis. First, unsupervised discriminant analysis was performed using principal component analysis (PCA) to remove outliers. Second, supervised partial least squares-discriminant analysis (PLS-DA) was performed, and the selected compound (variable importance in the projection: VIP >1), which made a significant contribution to the classification, was selected as the candidate marker. Finally, p value <0.05 was used to mark statistically significant differences, and potential biomarkers were identified using the m/z values of the markers, the Human Metabolome Database (HMDB) (http://www.hmdb.ca/) and the Kyoto Encyclopedia of Genes and Genomes (KEGG) (http://www.genome.jp/kegg/) database and the literature.

Systems biology analysis

To elucidate the effects of AgNP-cit on the metabolic pathways of rat liver, the KEGG database was used to integrate the proteomics and metabolomics results. Upon uploading the KEGG ID numbers and trends of the differentially expressed proteins and metabolites, the metabolic pathways associated with the differential proteins and metabolites were identified. We attempted to find correlations among the differentially expressed proteins and metabolites using Cytoscape_version 3.5.1 software

(National Institute of General Medical Sciences, Bethesda, MD) to establish molecular network maps.

Statistical analysis

SPSS version 17.0 (SPSS Inc., Chicago, IL) was used for statistical analysis. Statistical assessment was performed using Student's *t*-tests or Fisher's exact tests. The level of statistical significance was set at p value <0.05.

Results

Biochemical analysis and histopathological assessment

Detection and analysis of biochemical zymogram in serum is important for reflecting the degree of organ damage caused by toxic effects (Khalid and Ashraf 1993). Changes in serum levels of the biochemical indices aspartate aminotransferase (AST) and alanine aminotransferase (ALT) reflect damage to the liver caused by drugs to a certain extent. In this study, AST and ALT Student's *t*-test results in the control and AgNP-cit groups were compared to evaluate whether AgNP-cit caused liver damage (Figure 3). Results from the AgNP-cit group were significantly different (p value <0.01) than those of the control group, showing that AgNP-cit caused liver damage.

The histopathological results are shown in Figure 4. The basic structure of the liver in the control group was intact; the central vein was clearly visible, and no expansion or atrophy was observed. The AgNP-cit group showed tissue damage with infiltration (1–5%) around the portal area and central venous lymphocytes, obvious swelling and steatosis of the liver cells. Histopathological analysis showed that AgNP-cit caused pathological changes in the liver that led to damage, thus demonstrating that AgNP-cit results in liver toxicity.

Identification of differentially expressed proteins

The mass error of all the identified peptides was determined to perform the MS quality control test, revealing that the TMT-labeled quantitative proteomics method was stable, reliable, and reproducible.

To characterize changes in protein expression after AgNP-cit administration, the livers of rats in the control and AgNP-cit treatment groups were analyzed by the TMT-labeled quantitative proteomics method. In this study, a total of 5257 proteins were identified, 4631 of which contained quantitative information. Of the quantitative proteins, 130 showed significant differences ($p < 0.05$). The expression levels of 70 proteins in the AgNP-cit/control comparison group were up-regulated, and the expression levels of 60 proteins were down-regulated (Supplementary Table S3). The proteins with significantly differences altered expression showed that the protein spectrum in rat liver tissue is significantly altered by AgNP-cit.

To further understand the nature and biological functions of proteins, the identified differentially expressed proteins were classified and enriched by searching the gene ontology database (http://geneontology.org/) for biological process, cellular component and molecular function. Notably, the

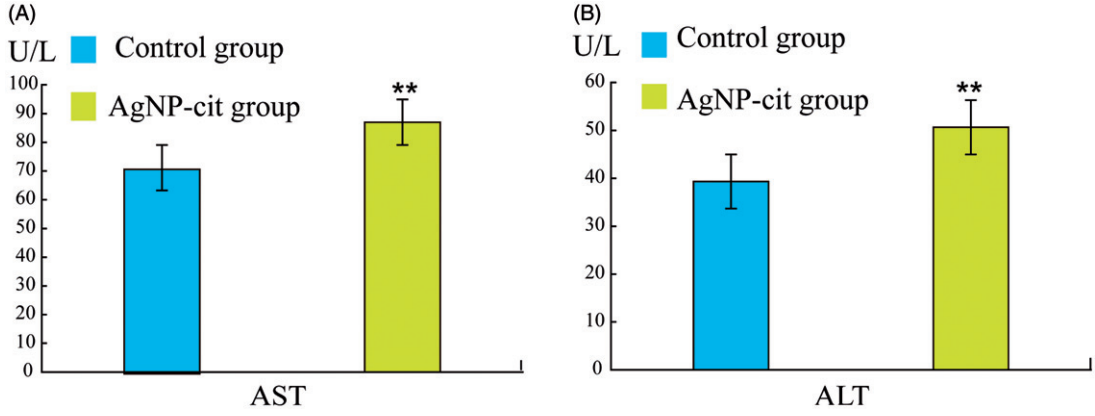

Figure 3. Content changes of AST (A) and ALT (B) in control group and AgNP-cit group. (A) Mean ± SD value of control group is 71.2 ± 2.4; mean ± SD value of AgNP-cit group is 87.0 ± 9.3; (B) Mean ± SD value of control group is 39.3 ± 2.5; Mean ± SD value of AgNP-cit group is 50.7 ± 2.7; **Compared with control group, there was very significant change (p value <0.01).

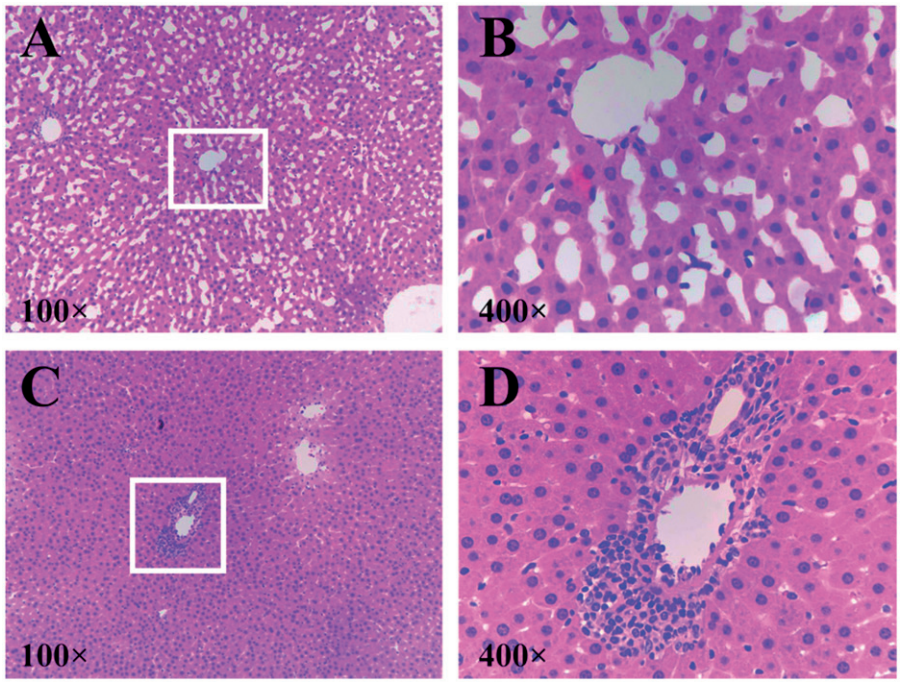

Figure 4. Histopathological sections of the liver. A and B are pathological sections of the control group with magnification of 100× and 400×, respectively. Control group without necrosis lesions; C and D are pathological sections of AgNP-cit group with magnification of 100× and 400×, respectively. AgNP-cit group: infiltration (1–5%) around the portal area and the central venous lymphocytes.

down-regulated proteins exhibit oxidoreductase activity, NAD + ADP-ribosyltransferase activity, NADPH binding, and other molecular functions. In addition, they are closely related to a variety of biological processes, including response to cytokines, metabolic processes and biosynthesis processes (Figure S1). Furthermore, AgNP-cit may cause liver damage by affecting redox balance, response to cytokines, and multiple metabolic pathways.

Screening metabolomics biomarkers

The MS quality control test was performed using instrument precision, method precision, and sample stability methodologies, among others. The results showed that the precision of the instrument was acceptable, the sample had good stability, and the method was reproducible.

In this experiment, metabolomics studies were performed using SIMCA-*P* + 11.5 multivariate statistical analysis software to gain information regarding the liver tissue samples, which were collected by UPLC/Q-TOF-MS. First, PCA was used for unsupervised data analysis. Figure 5(A) shows a good distinction between the administration and control groups, indicating that AgNP-cit caused changes in endogenous metabolites *in vivo*, and a clear distinction between the two groups was observed at the metabolic level. Second, based on the PLS-DA model, we further tapped potential information from the data. Variables with VIP >1 between the control and administration groups were selected as potential biomarkers associated with hepatotoxicity (Figure 5(B)). These markers were then subjected to Student's *t*-tests to identify significant changes (p value <0.05) in hepatotoxic biomarkers.

Finally, we identified 12 liver toxicity biomarkers. Specific ion information for these biomarkers (Table 2), includes mainly alanine, methionine, xanthine and other hepatotoxic biomarkers (Wang et al. 2012; Holecek 2013; Armagan et al. 2015; Sunny et al. 2015; Li et al. 2015, 2016; Yao et al. 2017). The metabolic pathways associated include mainly glycerol phospholipid metabolism, phenylalanine, tyrosine and tryptophan biosynthesis, purine metabolism and cysteine, and methionine metabolism, etc. Together, these results showed that AgNP-cit also significantly altered the metabolic profiles in the rat livers.

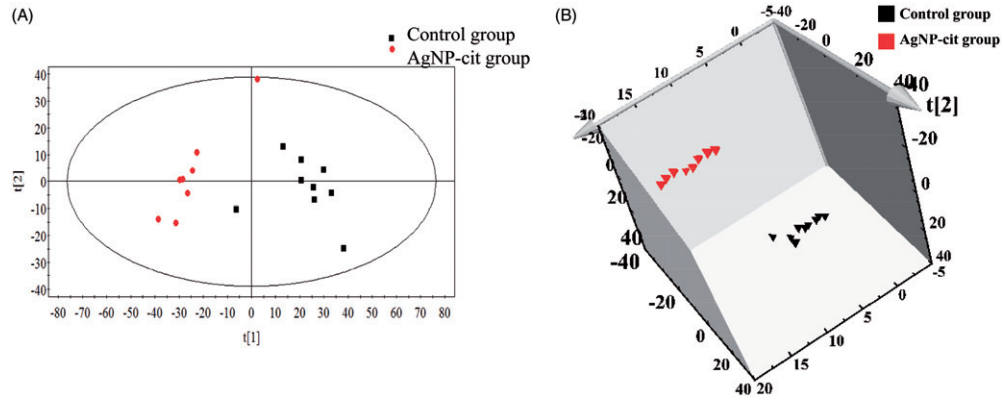

Figure 5. (A) PCA score chart of AgNP-cit group compared with Control group; (B) PLS-DA score chart of AgNP-cit group compared with Control group.

Table 2. The biomarker ion information of AgNP-cit group.

No.	t_R (min)	m/z Measured value	Metabolites	Molecular formula	Parent ion	Tendency	Fragment
1	2.1	90.0553	Alanine	$C_3H_7NO_2$	M + H	↓	90.0 $[M+H]^+$ 72.0 $[M+H-H_2O]^+$
2	2.0	132.1024	Alloisoleucine	$C_6H_{13}NO_2$	M + H	↓	132.1 $[M+H]^+$ 69.1 $[M+H-NH_3-HCOOH]^+$ 56.0 $[M+H-C_4H_{12}O]^+$ 86.1 $[M+H-C_3H_{10}]^+$
3	1.4	150.0586	Methionine	$C_5H_{11}NO_2S$	M + H	↓	150.1 $[M+H]^+$ 87.0 $[M+H-NH_3-HCOOH]^+$ 104.1 $[M+H-HCOOH]^+$ 133.0 $[M+H-NH_3]^+$
4	1.9	153.0411	Xanthine	$C_5H_4N_4O_2$	M + H	↓	153.0 $[M+H]^+$ 81.0 $[M+H-C_2H_4N_2O]^+$ 136.0 $[M+H-NH_3]^+$
5	8.8	182.082	Tyrosine	$C_9H_{11}NO_3$	M + H	↓	182.1 $[M+H]^+$ 136.1 $[M+H-HCOOH]^+$ 147.0 $[M+H-NH_3-H_2O]^+$ 165.1 $[M+H-NH_3]^+$
6	2.2	205.0978	Tryptophan	$C_{11}H_{12}N_2O_2$	M + H	↓	205.1 $[M+H]^+$ 159.1 $[M+H-HCOOH]^+$ 188.1 $[M+H-NH_3]^+$
7	5.1	494.3254	LPC(16:1)	$C_{24}H_{48}NO_7P$	M + H	↓	494.3 $[M+H]^+$ 476.3 $[M+H-H_2O]^+$ 184.1 $[M+H-C_{19}H_{34}O_3]^+$ 104.0 $[M+H-C_{19}H_{35}O_6P]^+$
8	6.5	468.3088	LPC(14:0)	$C_{22}H_{46}NO_7P$	M + H	↓	468.3 $[M+H]^+$ 450.3 $[M+H-H_2O]^+$ 184.1 $[M+H-C_{17}H_{32}O_3]^+$ 104.1 $[M+H-C_{17}H_{33}O_6P]^+$
9	5.5	520.341	LPC(18:2)	$C_{26}H_{50}NO_7P$	M + H	↓	520.3 $[M+H]^+$ 502.3 $[M+H-H_2O]^+$ 184.1 $[M+H-C_{21}H_{36}O_3]^+$ 104.1 $[M+H-C_{21}H_{37}O_6P]^+$
10	6.2	522.3568	LPC(18:1)	$C_{26}H_{52}NO_7P$	M + H	↓	522.4 $[M+H]^+$ 184.1 $[M+H-C_{21}H_{38}O_3]^+$ 104.1 $[M+H-C_{21}H_{39}O_6P]^+$
11	7.0	524.372	LPC(18:0)	$C_{26}H_{54}NO_7P$	M + H	↓	524.4 $[M+H]^+$ 184.1 $[M+H-C_{21}H_{40}O_3]^+$ 104.1 $[M+H-C_{21}H_{41}O_6P]^+$
12	5.7	534.2964	LPC(16:0)	$C_{24}H_{50}NO_7P$	M + K	↓	496.3 $[M+H]^+$ 184.0 $[M+H-C_{19}H_{36}O_3]^+$

Systems biology analysis

The proteomics results suggested that hepatotoxicity may have occurred, while the metabolomics results indicated that liver toxicity actually did occur. Combining the two analyses can explain the toxicity and toxic mechanisms that were demonstrated. Using the KEGG database, a network analysis of the complex metabolomics and proteomics

Table 3. Information table of 12 differential proteins obtained by integration analysis.

No.	KEGG KO No.	Protein description	Gene name	AgNP-cit/control ratio	Regulated type
1	K12406	Pyruvate kinase	*Pklr*	0.7700	Down
2	K17989	L-serine dehydratase/L-threonine deaminase	*Sds*	1.214	Up
3	K07424	Cytochrome P450 3A18	*Cyp3a18*	1.26	Up
4	K00006	Glycerol-3-phosphate dehydrogenase [NAD(+)], cytoplasmic	*Gpd1*	0.8220	Down
5	K00815	Tyrosine aminotransferase	*Tat*	0.7120	Down
6	K07424	Cytochrome P450 3A2	*Cyp3a2*	1.334	Up
7	K00456	Cysteine dioxygenase type 1	*Cdo1*	0.7870	Down
8	K00315	Dimethylglycine dehydrogenase, mitochondrial	*Dmgdh*	1.772	Up
9	K01080	Phosphatidic acid phosphatase type 2B	*Plpp3*	1.207	Up
10	K01837	Phosphoglycerate mutase	*Bpgm*	1.534	Up
11	K20838	N-acetyltransferase 8	*Nat8*	0.7630	Down
12	K00628	Glycine N-acyltransferase-like protein Keg1	*Keg1*	1.263	Up

Table 4. List of metabolic pathways involved in differential proteins and differential metabolites.

KEGG pathway	Name	*p* value	AgNP-cit/control ratio	Regulation
rno00564 Glycerophospholipid metabolism	Phosphatidic acid phosphatase type 2B	0.0023	1.207	Up
	Glycerol-3-phosphate dehydrogenase [NAD(+)]	0.0009	0.8220	Down
	Protein Etnppl	0.0000	1.446	Up
	LPC(18:0)	0.0001	0.1099	Down
	LPC(18:1)	0.0000	0.1270	Down
	LPC(16:0)	0.0001	0.1128	Down
	LPC(18:2)	0.0364	0.4035	Down
	LPC(14:0)	0.0003	0.0782	Down
	LPC(16:1)	0.0001	0.1386	Down
rno00400 Phenylalanine, tyrosine and tryptophan biosynthesis	Tyrosine aminotransferase	0.0049	0.7120	Down
	Tyrosine	0.0208	0.1994	Down
	Tryptophan	0.0000	0.2864	Down
rno00260 Glycine, serine and threonine metabolism	Dimethylglycine dehydrogenase, mitochondrial	0.0008	1.772	Up
	Phosphoglycerate mutase	0.0000	1.534	Up
	Pipecolic acid oxidase	0.0029	0.7970	Down
	L-serine dehydratase/L-threonine deaminase	0.0010	1.214	Up
	Tryptophan	0.0000	0.2864	Down
rno00270 Cysteine and methionine metabolism	Tyrosine aminotransferase	0.0049	0.7120	Down
	Cysteine dioxygenase type 1	0.0001	0.7870	Down
	L-serine dehydratase/L-threonine deaminase	0.0010	1.214	Up
	Methionine	0.0077	0.5048	Down
	Alanine	0.0000	0.2110	Down
rno00230 Purine metabolism	Pyruvate kinase	0.0000	0.7700	Down
	Xanthine	0.0108	0.7495	Down

data was conducted to find metabolic pathways and associations within the two datasets. In the end, we identified significant associations among between 12 differential proteins (Table 3) and 12 metabolites. The metabolic pathways involved are shown in Table 4, showing that the differential expression of proteins and metabolites in the liver was caused by the action of AgNP-cit. The differential expression of these proteins and metabolites affected glycerol phospholipid metabolism, phenylalanine, tyrosine and tryptophan biosynthesis, glycine, serine and threonine metabolism, cysteine and methionine metabolism, and purine metabolism, ultimately leading to liver damage.

Meanwhile, we used Cytoscape_version 3.5.1 software (National Institute of General Medical Sciences, Bethesda, MD) to create molecular network maps of differential proteins and metabolites (Figure 6). The figure shows relationships between the proteins and metabolites, revealing that glycerophospholipid metabolism, glycine, serine and threonine metabolism, purine metabolism, along with other metabolic pathways were changed due to the effects of AgNP-cit in liver tissue. Furthermore, the expression

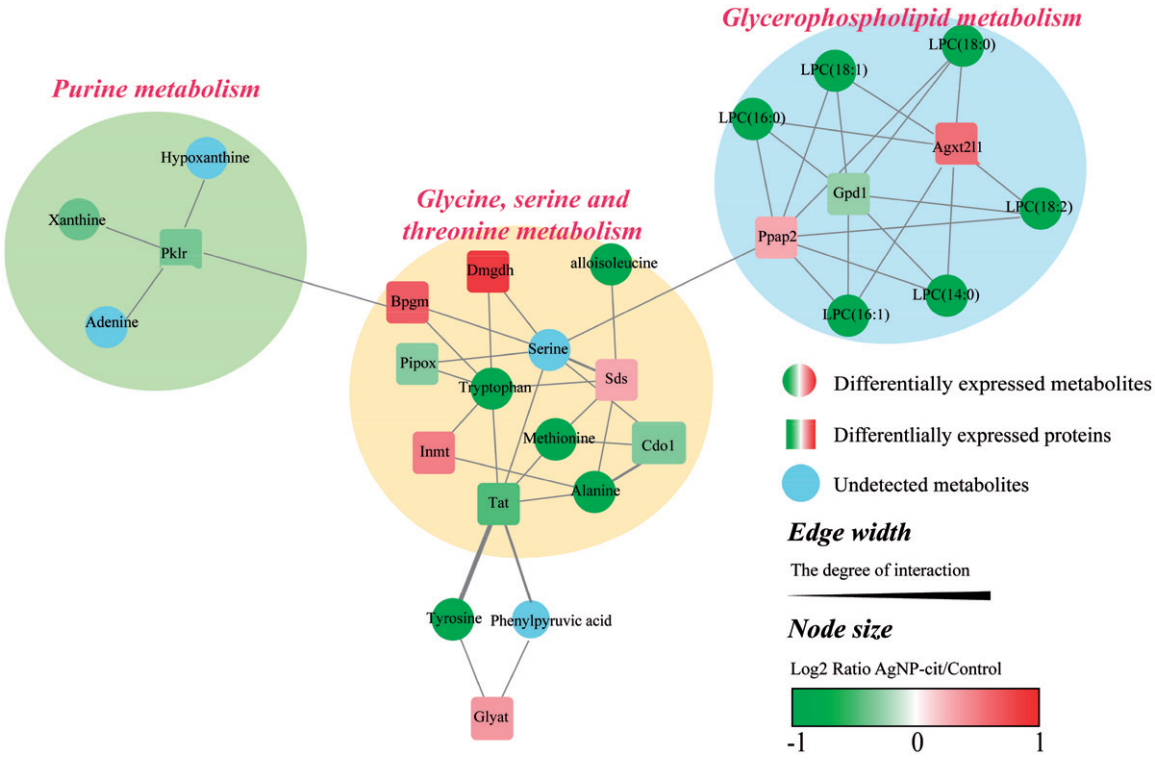

Figure 6. Molecular network of differentially expressed proteins and metabolites. The different edge widths represent the degree of interaction between the proteins and metabolites. The different color shades indicate the degree of variability in the altered metabolites or proteins.

of proteins and the content of metabolites downstream of these pathways are altered in liver tissue, inducing toxic reactions, and leading to liver damage.

Discussion

Mechanisms of AgNP-cit toxicity

Inflammatory responses, cellular DNA damage, oxidative stress and mitochondrial damage induced by AgNP-cit *in vitro* have been reported in literature. However, the information obtained from these assays is not sufficient to describe the information of system's biological reactions and key biochemical pathways induced by AgNP-cit on the organism. Systems biology methods, such as proteomics and metabolomics can identify key proteins and metabolites that are involved and more clearly explain the underlying biological mechanisms.

The differentially expressed proteins and metabolite molecular networks caused by AgNP-cit were identified using KEGG, and a toxicity mechanism map was designed (Figure 7). Hepatotoxicity induced by AgNP-cit involves multiple metabolic pathways in the body, and including glycerol phospholipid metabolism, purine metabolism, and cysteine and methionine metabolism. Three perspectives oxidative stress, inflammatory response, oxidation, and deamination, are discussed below to explain the mechanism underlying hepatotoxicity induced by AgNP-cit.

Oxidative stress

In this study, several differentially expressed proteins and metabolites were associated with oxidative stress and apoptosis. The levels of pyruvate kinase, N-acetyltransferase 8 (NAT8) and xanthine were down-regulated, while the level of glycine N-acyltransferase (GLYAT) was up-regulated in the AgNP-cit group compared to those in the control group. Pyruvate kinase (PK) plays an important role in the glycolytic pathway and in purine metabolism. The sugar channel is the main method providing energy for liver function and is essential for glucose metabolism. PK can catalyze the conversion of pyruvate phosphoenol (PEP) to pyruvate to produce adenosine triphosphate (ATP) during this period. Pyruvate kinase was significantly decreased after

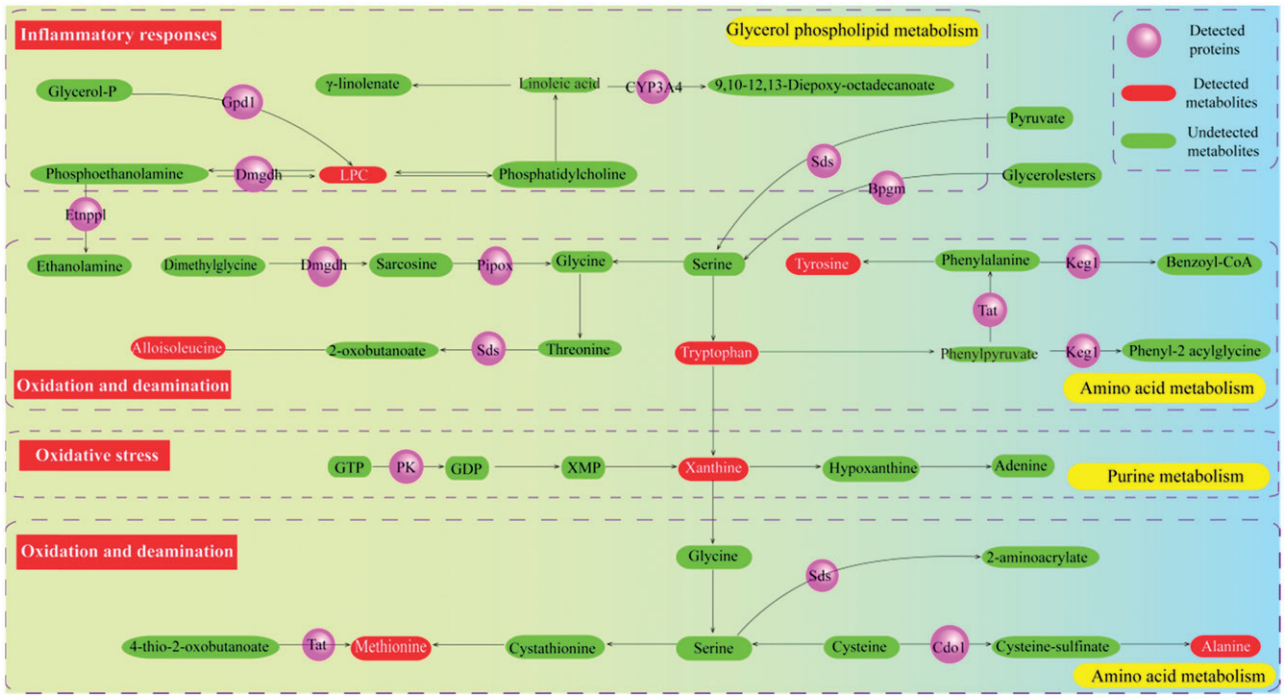

Figure 7. Mechanism diagram of liver toxicity induced by AgNP-cit.

AgNP-cit administration, affecting intracellular ATP levels, and potentially leading to apoptosis (Baldissera et al. 2015). In addition, adenosine has the role of regulating hepatic blood flow. Through a bodily feedback system, adenosine can be metabolized to adenine after phosphorylation. Adenine can form inosine after deamination, and inosine is then converted to hypoxanthine under the influence of purine nucleoside phosphorylase. Under the action of xanthine dehydrogenase, hypoxanthine is converted to xanthine. Meanwhile, guanosine triphosphate produces guanosine in the presence of pyruvate kinase, and guanosine is phosphorylated to produce guanine, and is then converted to xanthine. Xanthine, a substrate for xanthine dehydrogenase, is associated with the level of oxidative stress in the body. Xanthine is metabolized to uric acid and hypoxanthine under the catalysis of xanthine dehydrogenase (Armagan et al. 2015). During catalytic process, the catalytic production of reactive oxygen species (ROS) increased the level of oxidative stress in the body, and the oxidation and antioxidant systems were imbalanced, directly causing liver cell damage.

NAT8, a cysteinyl-conjugated N-acetyltransferase, is a microsomal enzyme that catalyzes the final step of mercapto acids formation, which is significant for the detoxification and excretion of cysteinyl conjugates (Veiga-da-Cunha et al. 2010). AgNP-cit acted on the body to down-regulate NAT8, which has been reported to potentially aggravate hepatocyte apoptosis. When liver cells are damaged, cellular oxidative stress leads to the oligomerization of glutathione transferase, which decreases NAT8 levels and activates the MAPK/JNK pathway, ultimately leading to apoptosis (Fu et al. 2014). Proteomics analysis showed that GLYAT, which participates in oxidative stress in the liver and plays a key role in the process of hepatocyte differentiation and nitrogen metabolism *in vivo* (Matsuo et al. 2012), was elevated after AgNP-cit administration. Furthermore, GLYAT reportedly transfers an acyl group to glycine amino terminus, binds bile acids to taurine or glycine and localizes in peroxisomes and microsomes. AgNP-cit administration resulted in abnormal GLYAT expression, which could cause liver damage. Together, these data showed that AgNP-cit significantly altered the levels of PK, NAT8, GLYAT and xanthine, leading to purine metabolism abnormalities and ultimately resulting in liver damage by oxidative stress.

Inflammatory responses

In this study, cytochrome P450, dimethylglycine dehydrogenase, and phosphatidic acid phosphatase

were up-regulated, while tyrosine, tryptophan, glycerophospholipids, tyrosine aminotransferase, and glycerol-3-phosphate dehydrogenase were down-regulated in the liver after AgNP-cit was administered to rats. Under the influence of cytochrome P450, drugs in the liver can induce reactions, such as oxidation, reduction, hydrolysis, and binding, etc. Electrophilic or oxygen-free radical metabolites, produced in the action of CYP450 and drugs, induce chemical reactions with cell membrane, and CYP450 metabolites react with DNA and a variety of protein molecules, leading to liver damage (Lu et al. 2017). Metal nanoparticles can reportedly alter the expression and function of CYP450 and various inflammatory cytokines have a certain degree of selectivity for specific CYP isoforms (Tang et al. 2016). In addition, imbalance between proinflammatory cytokines and anti-inflammatory cytokines may cause liver damage. Nguyen et al. (2013) found that silver nanoparticles have either a stimulatory or inhibitory effect on the production of cytokines, and modified silver nanoparticles appear to induce cell damage through inflammatory pathways by up-regulating cytokines.

Tyrosine, a major component of aromatic amino acids, is mainly metabolized in the cytoplasm of liver cells and is well-correlated with liver damage (Suzuki et al. 1998). AgNP-cit acted on the body, decreasing the level of tyrosine and disrupting tyrosine metabolism, which may lead to liver damage. Tyrosine aminotransferase (Tat) has a significant effect on tyrosine catabolism and was down-regulated due to the toxic effects of AgNP-cit. This led to accumulation of tyrosine and its by-products, which may damage the liver (Fu et al. 2010). Tryptophan has demonstrated an extraordinary ability to reduce the levels of proinflammatory cytokines in the treatment of liver disease (Li et al. 2016). In this study, the level of tryptophan was significantly reduced due to AgNP-cit, resulting in its decreased ability to reduce proinflammatory cytokine levels, ultimately inducing inflammation liver damage.

Choline is a constituent of lecithin and the precursor of acetylcholine, and two choline metabolic pathways may exist. On the one hand, choline can phosphorylate phosphorylcholine and participate in the biosynthesis of phosphatidylcholine. On the other hand, choline can be converted to glycine by dimethylglycine dehydrogenase and sarcosine dehydrogenase. Furthermore, phosphatidate phosphohydrolase can reportedly promote the synthesis of phosphatidylcholine, phosphatidylethanolamine and triacylglycerol (Simpson et al. 1989). Glycerol-3-phosphate is a key metabolite in the translocation of reducing power through mitochondrial glycerol-3-phosphate dehydrogenase. At the same time, glycerol-3-phosphate dehydrogenase, as a major link between carbohydrate metabolism and lipid metabolism, catalyzes the formation of ethanolamine lysophospholipids (Taleux et al. 2009). Glycerol phospholipids are highly biologically active molecules that are involved in inflammatory responses. When the liver is damaged, the expression of cytokine receptors in immune cells, including monocytes, macrophages and dendritic cells is inhibited. With increasing degrees of liver damage, the amounts of cytokines decreases, resulting in decreased liver synthesis, metabolism, and transformation functions. This study showed that the levels of tyrosine, tryptophan, and glycerophospholipid metabolites were reduced and tyrosine aminotransferase, and glycerol-3-phosphate dehydrogenase also showed a downward trend. These affects blocked the biosynthesis of phenylalanine, tyrosine and tryptophan and gave rise to abnormal glycerol phospholipid metabolism, which led to inflammatory reactions and liver damage.

Oxidation and deamination

In this study, compared with those of control group, the levels of L-serine dehydratase/L-threonine deaminase and phosphoglycerate mutase were up-regulated, while cysteine dioxygenase, alanine, isoleucine, and methionine were down-regulated. L-threonine deaminase is an enzyme in the liver that is responsible for the conversion of L-threonine to α-ketobutyric acid and ammonia. Because α-ketoester can be converted to isoleucine, L-threonine deaminase plays a key role in the synthesis of branched-chain amino acids (Du et al. 2014). Moreover, serine dehydratase and phosphoglycerate mutase 1 catalyze pyruvate and glycerol ester, respectively, to generate serine, thereby producing isoleucine. Isoleucine is a branched chain amino acid, and the carbon skeleton required for its

synthesis is derived from the intermediate products of anaerobic and aerobic sugar metabolism. In this research, under the toxic effects of AgNP-cit, the level of isoleucine were potentially down-regulated by L-serine dehydratase/L-threonine deaminase and phosphoglycerate mutase, which disrupted amino acid metabolism and led to liver damage.

Cysteine catabolism mainly proceeds the oxidation of cysteine sulfate. In the cysteine dioxygenase (CDO) catalytic reaction, dioxyl is added to cysteine to form a cysteine sulfinic acid, which is further converted to alanine (Ueki et al. 2011). Alanine enters the liver through the blood, combining with deamination and releasing ammonia to synthesize urea, which is an important biological function of liver cells. Since AgNP-cit decreases the alanine content, urea synthesis is obstructed in the liver, causing liver damage (Su et al. 2017). Meanwhile, the methionine content was significantly reduced in the cysteine and methionine metabolic pathways, suggesting that cysteine and methionine metabolism was abnormal and that the liver was seriously injured by the effects of AgNP-cit (Dominy, Hwang, and Stipanuk 2007). AgNP-cit up-regulated L-serine dehydratase/L-threonine deaminase and phosphoglycerate mutase, and down-regulated cysteine dioxygenase, alanine, isoleucine and methionine in the liver, which are involved in oxidation, and deamination. This led to abnormalities of glycine, serine and threonine metabolism, cysteine, and methionine metabolism, thus resulting in liver damage.

Conclusions

Omics techniques are characterized by the qualitative and quantitative analysis of a wide range of biomolecules. Proteomics can reveal changes in protein spectra caused by exposure to nanomaterials (Su et al. 2013; Roy, Goswami, and Pal 2016). Metabolomics identifies key metabolites associated with exposure to nanomaterials. The combination of the two can explain the biological mechanisms of drug toxicity more accurately and systematically. Thus, in this study, a combination of proteomics and metabolomics was used to reveal the toxic mechanisms of AgNP-cit-induced liver damage. The results suggested that AgNP-cit caused purine metabolism abnormalities mainly by affecting the contents of xanthine and other key metabolites along with pyruvate kinase and other proteins in the body, leading to oxidative stress. AgNP-cit can regulate the metabolism of amino acids and glycerol phospholipids through glycerol phospholipids, other metabolites, CYP450 enzymes, and other key proteins, thus causing inflammation in the liver. Through alanine, isoleucine, L-serine dehydratase/L-threonine deaminase, and other proteins, AgNP-cit caused abnormal metabolisms of glycine, serine and threonine, cysteine and methionine, leading to liver damage. AgNP-cit led to toxic reactions in the liver mainly altering the contents of 12 proteins and 12 metabolites differentially expressed in the liver, causing oxidative stress, inflammatory response, oxidation, and deamination, leading to toxic reactions of the liver. This research provides a detailed explanation of the hepatotoxicity mechanism of AgNP-cit, which provides not only a reference for the toxic mechanism of AgNP-cit but also a basis for the safe application of nanomaterials.

Disclosure statement

The authors report that they have no conflicts of interest.

Funding

This project was supported by Program for Changjiang Scholars and Innovative Research Team in University (IRT_14R41).

References

Agnihotri, S., S. Mukherji, and S. Mukherji. 2014. "Size-Controlled Silver Nanoparticles Synthesized over the Range 5–100 nm Using the Same Protocol and Their Antibacterial Efficacy." *RSC Advances* 4 (8): 3974–3983. doi:10.1039/C3RA44507K.

Armagan, I., D. Bayram, I. A. Candan, A. Yigit, E. Celik, H. H. Armagan, and A. C. Uğuz. 2015. "Effects of Pentoxifylline and Alpha Lipoic Acid on Methotrexate-Induced Damage in Liver and Kidney of Rats." *Environmental Toxicology and Pharmacology* 39 (3): 1122–1131. doi:10.1016/j.etap.2015.04.003.

Bai, Y., H. Zhang, X. Sun, C. Sun, and L. Ren. 2014. "Biomarker Identification and Pathway Analysis by Serum Metabolomics of Childhood Acute Lymphoblastic Leukemia." *Clinica Chimica Acta* 436: 207–216. doi:10.1016/j.cca.2014.05.022.

Baldissera, M. D., N. B. Bottari, R. E. Mendes, C. I. Schwertz, N. J. Lucca, D. Dalenogare, G. V. Bochi, R. N. Moresco, V. M. Morsch, and M. R. Schetinger. 2015. "Activity of Cholinesterases, Pyruvate Kinase and Adenosine Deaminase in Rats Experimentally Infected by *Fasciola hepatica*: Influences of These Enzymes on Inflammatory Response and Pathological Findings." *Pathology-Research and Practice* 211: 871–876. doi:10.1016/j.prp.2015.09.006.

Bastos, V., J. F. De Oliveira, D. Brown, H. Jonhston, E. Malheiro, A. Daniel-Da-Silva, I. Duarte, C. Santos, and H. Oliveira. 2016. "The Influence of Citrate or PEG Coating on Silver Nanoparticle Toxicity to a Human Keratinocyte Cell Line." *Toxicology Letters* 249: 29–41. doi:10.1016/j.toxlet.2016.03.005.

Dominy, J. E., J. Hwang, and M. H. Stipanuk. 2007. "Overexpression of Cysteine Dioxygenase Reduces Intracellular Cysteine and Glutathione Pools in HepG2/C3A Cells." *American Journal of Physiology-Endocrinology and Metabolism* 293 (1): E62–E69. doi:10.1152/ajpendo.00053.2007.

Du, Y., L. Hong, W. Tang, L. Li, X. Wang, H. Ma, Z. Wang, H. Zhang, X. Zheng, and Z. Zhang. 2014. "Threonine Deaminase Mollv1 is Important for Conidiogenesis and Pathogenesis in the Rice Blast Fungus Magnaporthe Oryzae." *Fungal Genetics and Biology* 73: 53–60. doi:10.1016/j.fgb.2014.10.001.

Fu, J., H. Zhang, Y. Zhuang, H. Liu, Q. Shi, D. Li, X. Ju, and S. Gronthos. 2014. "The Role of N-Acetyltransferase 8 in Mesenchymal Stem Cell-Based Therapy for Liver Ischemia/Reperfusion Injury in Rats." *PLoS One* 9 (7): e103355. doi:10.1371/journal.pone.0103355.

Fu, L., S. S. Dong, Y. W. Xie, L. S. Tai, L. Chen, K. L. Kong, K. Man, et al. 2010. "Down-regulation of Tyrosine Aminotransferase at a Frequently Deleted Region 16q22 Contributes to the Pathogenesis of Hepatocellular Carcinoma." *Hepatology* 51 (5): 1624. doi:10.1002/hep.23540.

Holecek, M. 2013. "Branched-chain Amino Acids and Ammonia Metabolism in Liver Disease: Therapeutic Implications." *Nutrition* 29 (10): 1186–1191. doi:10.1016/j.nut.2013.01.022.

Hussain, S., K. Hess, J. Gearhart, K. Geiss, and J. Schlager. 2005. "In Vitro Toxicity of Nanoparticles in BRL 3A Rat Liver Cells." *Toxicology in Vitro : An International Journal Published in Association with Bibra* 19 (7): 975–983. doi:10.1016/j.tiv.2005.06.034.

Jiménez-Lamana, J., F. Laborda, E. Bolea, I. Abad-Álvaro, J. R. Castillo, J. Bianga, M. He, et al. 2014. "An Insight into Silver Nanoparticles Bioavailability in Rats." *Metallomics* 6 (12): 2242–2249. doi:10.1039/C4MT00200H.

Khadzhynov, D., C. Schelter, I. Lieker, A. Mika, O. Staeck, H. H. Neumayer, H. Peters, and T. Slowinski. 2014. "Incidence and Outcome of Metabolic Disarrangements Consistent with Citrate Accumulation in Critically Ill Patients Undergoing Continuous Venovenous Hemodialysis with Regional Citrate Anticoagulation." *Journal of Critical Care* 29 (2): 265–271. doi:10.1016/j.jcrc.2013.10.015.

Khalid, M. A., and M. Ashraf. 1993. "Direct Detection of Endogenous Hydroxyl Radical Production in Cultured Adult Cardiomyocytes During Anoxia and Reoxygenation. Is the Hydroxyl Radical Really the Most Damaging Radical Species?" *Circulation Research* 72 (4): 725–736. doi:10.1161/01.RES.72.4.725.

Kuzmanov, U., H. Guo, D. Buchsbaum, J. Cosme, C. Abbasi, R. Isserlin, P. Sharma, A. O. Gramolini, and A. Emili. 2016. "Global Phosphoproteomic Profiling Reveals Perturbed Signaling in a Mouse Model of Dilated Cardiomyopathy." *Proceedings of the National Academy of Sciences* 113 (44): 12592–12597. doi:10.1073/pnas.1606444113.

Lavatelli, F., and G. Merlini. 2016. "Advances in Proteomic Study of Cardiac Amyloidosis: Progress and Potential." *Expert Review of Proteomics* 13 (11): 1017–1027. doi:10.1080/14789450.2016.1242417.

Li, Y., L. Wang, L. Ju, H. Deng, Z. Zhang, Z. Hou, J. Xie, Y. Wang, and Y. Zhang. 2016. "A Systematic Strategy for Screening and Application of Specific Biomarkers in Hepatotoxicity Using Metabolomics Combined with ROC Curves and SVMs." *Toxicological Sciences* 150 (2): 390–399. doi:1toxsci/toxsci/kfw001.

Li, Y., Z. Zhang, X. Liu, A. Li, Z. Hou, Y. Wang, and Y. Zhang. 2015. "A Novel Approach to the Simultaneous Extraction and Non-Targeted Analysis of the Small Molecules Metabolome and Lipidome Using 96-Well Solid Phase Extraction Plates with Column-Switching Technology." *Journal of Chromatography A* 1409: 277–281. doi:10.1016/j.chroma.2015.07.048.

Licker, V., N. Turck, E. Kövari, K. Burkhardt, M. Côte, M. Surini-Demiri, J. A. Lobrinus, J. C. Sanchez, and P. R. Burkhard. 2014. "Proteomic Analysis of Human Substantia Nigra Identifies Novel Candidates Involved in Parkinson's Disease Pathogenesis." *Proteomics* 14 (6): 784–794. doi:10.1002/pmic.201300342.

Lin, J. 2008. *Metabonomics Study on Chemical Liver Injury and Liver Cancer*. Shanghai: Shanghai Jiao Tong University.

Lu, J., Y. Shao, X. Qin, D. Liu, A. Chen, D. Li, M. Liu, and X. Wang. 2017. "CRISPR Knockout Rat Cytochrome P450 3A1/2 Model for Advancing Drug Metabolism and Pharmacokinetics Research." *Scientific Reports* 7: 42922. doi:10.1038/srep42922.

Matsuo, M., K. Terai, N. Kameda, A. Matsumoto, Y. Kurokawa, Y. Funase, K. Nishikawa, N. Sugaya, N. Hiruta, and T. Kishimoto. 2012. "Designation of Enzyme Activity of Glycine-N-Acyltransferase Family Genes and Depression of Glycine-N-Acyltransferase in Human Hepatocellular Carcinoma." *Biochemical and Biophysical Research Communications* 420 (4): 901–906. doi:10.1016/j.bbrc.2012.03.099.

Nguyen, K. C., V. L. Seligy, A. Massarsky, T. W. Moon, P. Rippstein, J. Tan, and A. F. Tayabali. 2013. "Comparison of Toxicity of Uncoated and Coated Silver Nanoparticlesed."

Journal of Physics: Conference Series 950: 265–278. doi:10.1088/issn.1742-6596.

Piao, M. J., K. A. Kang, I. K. Lee, H. S. Kim, S. Kim, J. Y. Choi, J. Choi, and J. W. Hyun. 2011. "Silver Nanoparticles Induce Oxidative Cell Damage in Human Liver Cells through Inhibition of Reduced Glutathione and Induction of Mitochondria-involved Apoptosis." *Toxicology Letters* 201 (1): 92–100. doi:10.1016/j.toxlet.2010.12.010.

Qin, G., S. Tang, S. Li, H. Lu, Y. Wang, P. Zhao, B. Li, J. Zhang, and L. Peng. 2017. "Toxicological Evaluation of Silver Nanoparticles and Silver Nitrate in Rats Following 28 Days of Repeated Oral Exposure." *Environmental Toxicology* 32 (2): 609–618. doi:10.1002/tox.22263.

Recordati, C., M. De Maglie, S. Bianchessi, S. Argentiere, C. Cella, S. Mattiello, F. Cubadda, et al. 2016. "Tissue Distribution and Acute Toxicity of Silver After Single Intravenous Administration in Mice: Nano-Specific and Size-Dependent Effects." *Particle and Fibre Toxicology* 13 (1): 12. doi:10.1186/s12989-016-0124-x.

Roy, D. N., R. Goswami, and A. Pal. 2016. "Nanomaterial and Toxicity: What Can Proteomics Tell Us about the Nanotoxicology?" *Xenobiotica: The Fate of Foreign Compounds in Biological Systems* 47: 1. doi:10.1080/00498254.

Simpson, K., S. Venkatesan, T. Peters, A. Martin, and D. Brindley. 1989. *Hepatic Phosphatidate Phosphohydrolase Activity in Acute and Chronic Alcohol-Fed Rats*. London: Portland Press Limited.

Stringer, K. A., R. T. Mckay, A. Karnovsky, B. Quémerais, and P. Lacy. 2016. "Metabolomics and Its Application to Acute Lung Diseases." *Frontiers in Immunology* 7: 44. doi:10.3402/jchimp.v4.24927.

Su, G., G. Chen, X. An, H. Wang, and Y. H. Pei. 2017. "Metabolic Profiling Analysis of the Alleviation Effect of Treatment with Baicalin on Cinnabar Induced Toxicity in Rats Urine and Serum." *Frontiers in Pharmacology* 8: 271. doi:10.3389/fphar.2017.00271.

Su, C. L., T. T. Chen, C. C. Chang, K. J. Chuang, C. K. Wu, W. T. Liu, K. F. Ho, K. Y. Lee, S. C. Ho, and H. E. Tseng. 2013. "Comparative Proteomics of Inhaled Silver Nanoparticles in Healthy and Allergen Provoked Mice." *International Journal of Nanomedicine* 8: 2783. doi:10.2147/IJN.S46997.

Sunny, N. E., S. Kalavalapalli, F. Bril, T. J. Garrett, M. Nautiyal, J. T. Mathew, C. M. Williams, and K. Cusi. 2015. "Cross-talk between Branched-chain Amino Acids and Hepatic Mitochondria is Compromised in Nonalcoholic Fatty Liver Disease." *American Journal of Physiology – Endocrinology and Metabolism* 309 (4): E311–E319. doi:10.1152/ajpendo.00161.2015.

Suzuki, H., Y. Mamata, H. Mizuno, T. Tominaga, M. Suga, S. Suemori, A. Sato, and M. Suzuki. 1998. "Influence of Alcohol on Branched-chain Amino Acid/Tyrosine Molar Ratio in Patients with Cirrhosis." *Alcoholism, Clinical and Experimental Research* 22 (1): 137S–140S. doi:10.1097/00000374-199803001-00013.

Taleux, N., B. Guigas, H. Dubouchaud, M. Moreno, J. M. Weitzel, F. Goglia, R. Favier, and X. M. Leverve. 2009. "High Expression of Thyroid Hormone Receptors and Mitochondrial Glycerol-3-Phosphate Dehydrogenase in the Liver is Linked to Enhanced Fatty Acid Oxidation in Lou/C, a Rat Strain Resistant to Obesity." *Journal of Biological Chemistry* 284 (7): 4308–4316. doi:10.1074/jbc.M806187200.

Tang, H. Q., M. Xu, Q. Rong, R. W. Jin, Q. J. Liu, and Y. L. Li. 2016. "The Effect of ZnO Nanoparticles on Liver Function in Rats." *International Journal of Nanomedicine* 11: 4275–4285. doi:10.2147/IJN.S109031.

Tiwari, D. K., T. Jin, and J. Behari. 2011. "Dose-dependent In-Vivo Toxicity Assessment of Silver Nanoparticle in Wistar Rats." *Toxicology Mechanisms and Methods* 21 (1): 13–24. doi:10.3109/15376516.2010.529184.

Ueki, I., H. B. Roman, A. Valli, K. Fieselmann, J. Lam, R. Peters, L. L. Hirschberger, and M. H. Stipanuk. 2011. "Knockout of the Murine Cysteine Dioxygenase Gene Results in Severe Impairment in Ability to Synthesize Taurine and an Increased Catabolism of Cysteine to Hydrogen Sulfide. American Journal of Physiology." *Endocrinology and Metabolism* 301 (4): E668–E684. doi:10.1152/ajpendo.00151.2011.

Veiga-Da-Cunha, M., D. Tyteca, V. Stroobant, P. J. Courtoy, F. R. Opperdoes, and E. Van Schaftingen. 2010. "Molecular Identification of NAT8 as the Enzyme That Acetylates Cysteine S-conjugates to Mercapturic Acids." *Journal of Biological Chemistry* 285 (24): 18888–18898. doi:10.1074/jbc.M110.110924.

Wang, X., A. Zhang, Y. Han, P. Wang, H. Sun, G. Song, T. Dong, et al. 2012. "Urine Metabolomics Analysis for Biomarker Discovery and Detection of Jaundice Syndrome in Patients with Liver Disease." *Molecular & Cellular Proteomics* 11 (8): 370–380. doi:10.1074/mcp.M111.016006.

Wei, L., J. Lu, H. Xu, A. Patel, Z. S. Chen, and G. Chen. 2015. "Silver Nanoparticles: Synthesis, Properties, and Therapeutic Applications." *Drug Discovery Today* 20 (5): 595–601. doi:10.1016/j.drudis.2014.11.014.

Xu, H., X. Chen, X. Xu, R. Shi, S. Suo, K. Cheng, Z. Zheng, et al. 2016. "Lysine Acetylation and Succinylation in HeLa Cells and Their Essential Roles in Response to UV-induced Stress." *Scientific Reports* 6 (1): 30212. doi:10.1038/srep30212.

Yao, Y., P. Zhang, J. Wang, J. Chen, Y. Wang, Y. Huang, Z. Zhang, and F. Xu. 2017. "Dissecting Target Toxic Tissue and Tissue Specific Responses of Irinotecan in Rats Using Metabolomics Approach." *Frontiers in Pharmacology* 8: 122. doi:10.3389/fphar.2017.00122.